The influence of surface functionalisation on the electrical properties and thermal stability of nanodiamonds

Joseph O Welch, Pei Li, Aysha Chaudhary, Robert Edgington, and Richard B. Jackman

---

Articles you may be interested in

Electrical properties and thermal stability of Pd-doped copper nitride films
J. Appl. Phys. **113**, 043705 (2013); 10.1063/1.4788905

Influence of a-Si:H deposition power on surface passivation property and thermal stability of a-Si:H/SiNx:H stacks
AIP Advances **2**, 022106 (2012); 10.1063/1.3703659

Bulk and surface thermal stability of ultra nanocrystalline diamond films with 10–30 nm grain size prepared by chemical vapor deposition
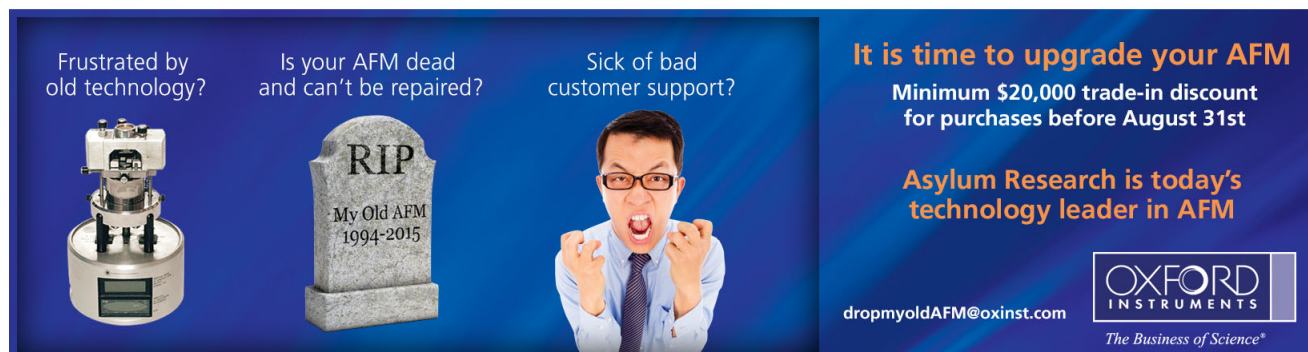J. Appl. Phys. **107**, 093521 (2010); 10.1063/1.3359714

Thermal stability comparison of TaN on HfO 2 and Al 2 O 3
Appl. Phys. Lett. **96**, 151907 (2010); 10.1063/1.3396189

Thermal imidization of fluorinated poly(amic acid) precursors on a glycidyl methacrylate graft-polymerized Si(100) surface
J. Vac. Sci. Technol. A **19**, 547 (2001); 10.1116/1.1340653

The influence of surface functionalisation on the electrical properties and thermal stability of nanodiamonds

Joseph O Welch, Pei Li, Aysha Chaudhary, Robert Edgington, and Richard B. Jackman[a)]
London Centre for Nanotechnology and the Department of Electronic and Electrical Engineering,
University College London, 17-19 Gordon Street, London WC1H 0AH, United Kingdom

Detonation nanodiamond (ND) has recently emerged as a useful new class of diamond material. However, to date there has been little investigation of the electrical properties of this material. Due to the nanoscale dimensions, the surface functionalisation of the individual ND is of particular importance to the characteristics of ND films. Here, hydrogen and oxygen termination of ND, verified using Fourier transform infrared spectroscopy, are shown to strongly influence the electronic properties of NDs. Hydrogen terminated ND exhibiting a far greater resilience to thermal decomposition when compared to the oxygen terminated NDs. Moreover, H-NDs also displayed so-called "surface conductivity," a property displayed by hydrogen-terminated bulk diamond films, whilst O-NDs display properties high resistivity. These results indicate that under the correct conditions ND layers can display similar electrical properties to "bulk" diamond thin films. © 2014 Author(s). All article content, except where otherwise noted, is licensed under a Creative Commons Attribution 3.0 Unported License. [http://dx.doi.org/10.1063/1.4897218]

I. INTRODUCTION

Diamond surfaces can support a wide range of functional chemical groups. These include, but are not limited to, hydrogen, hydroxide, oxygen, esters, carboxyl, amines, silane, and halogens.[1] The ultra-low dimensions of nanodiamonds formed by detonation processes (ND), being typically around 5 nm,[2] result in the constituent atoms being largely at the surface, therefore functionalisation of the surface can have a large effect on the characteristics of single digit NDs. The electrical properties of ND layers in the presence of functional groups are not well understood. Whilst the current and future range of applications for NDs is vast, only a small amount of work has focused on the study of their electrical properties. In work presented by Chaudhary *et al.*,[3] resistivity of untreated ND layers was found to be similar to that of bulk diamond. Additionally, the dielectric character of the ND layers was also found to be good, with dielectric loss tangent values found to lie between 0.05 and 0.5. These values were found to be permanently lost after 10 min of heating at 425 °C. Kondo *et al.* found the electrical conductivity of ND powder packed into a glass cylinder with an internal diameter of 1 mm to be reduced by almost 2 orders of magnitude after hydrogen termination.[4] This work aims to improve the current level of understanding of the electrical properties of ND with differing surface functional groups. Impedance spectroscopy (IS) was performed on ND layers in a sandwich (or parallel plate stack) configuration across a wide temperature range. This was done in order to study thermal stability and the progression of temperature dependant electrical characteristics. Additional experiments were performed in vacuum in order to provide a comparison against the effect of air on the decomposition of the NDs constituent components,

and to prevent adsorbates from the air providing the electron sink needed for so-called surface conductivity.[5] Oxygen and hydrogen functionalisations were chosen due to the previously reported large observed changes in surface conductivity,[6,7] electron affinity,[8] hydrophobicity/hydrophilicity,[9] and thermal stability[10,11] seen in various forms of diamond. IS was employed for this study due to its previously demonstrated suitability of electrically investigating nano- and microcrystalline materials—including diamond.[12,13] IS is of particular use in this instance, as it can be used for the deconvolution of multiple conduction paths seen in complex arrangements of diamond and carbon materials, as has been previously well established.[14,15]

II. EXPERIMENTAL METHODS

Sample preparation: Monodispersed detonation-derived nanodiamond (DND) colloid, NanoAmando, was used throughout (New Metals & Chemicals Corporation, Japan). This form of DND has been subjected to a deagglomeration process utilising wet milling with zirconia.[16] In order to perform IS through (rather than across) the ND layer a sandwich arrangement was employed, using an ND coating on one side polished (at the ND-silicon interface), highly conductive silicon (arsenic doped, $\rho = 0.001$ Ω.cm) seeded with ~10 nm thick layer of ND as described previously.[2] *Hydrogen anneal treatment*: A custom made chamber was used to heat samples to 500 °C in 10 Torr of hydrogen for 5 h and allowed to cool in hydrogen. *Ozone treatment*: A custom built chamber was used in conjunction with a commercially available ozone generation unit (Ozonia TOGC2–100201). Here, samples were subjected to ozone flow at a pressure of 50 mbar, at 200 °C for 30 min. After which the sample was allowed to cool in ozone before being removed. *Impedance spectroscopy*: Measurements were made by taking the coated

---

a)Author to whom correspondence should be addressed. Electronic mail: r.jackman@ucl.ac.uk.

116, 133705-1

DND substrates and placing them inside a Solartron 1260 Impedance measurement system. This system was also integrated with a Solartron 1296 Dielectric Interface in order to measure the high impedance anticipated (the 1296 in conjunction with the 1260 is specified to the range of $100 - 10^{14}\,\Omega$ and $0.1 - 10^7\,Hz$).[17] The sample was placed on a ceramic heater inside a vacuum chamber (to provide electrical and environmental isolation), connected to the impedance equipment. Two metal probes were then placed on the top and bottom plates in order to probe through the ND layer, as described elsewhere.[2] Measurements were then taken either at atmospheric pressure or vacuum ($10^{-2} - 10^{-3}$ mbar), across a temperature range from room temperature to a maximum of $580\,^{\circ}C$, where the temperature was maintained for 10 min unless otherwise specified. If during the course of taking a heated measurement there was significant change in the magnitude of the impedance, the sample was then cooled to room temperature and retested. Control measurements were taken using uncoated silicon plates to ensure the effects observed were due to the ND layers. Samples were tested until destruction or the limits of the measurement equipment (e.g., loss of resistivity or gain in noise) or heater assembly were reached. *FTIR:* FTIR spectroscopy was performed using a Perkin Elmer Spectrum One FTIR Spectrometer. Samples were either directly drop coated onto (when in solution) or scraped from the treatment substrate onto CaF_2 windows for analysis. Drop coating was performed in a clean room environment by pipetting one drop at a time of concentrated solution onto CaF_2 windows placed a bench top heater set to $\sim 100\,^{\circ}C$. Scrape coated windows had a similar volume of ND to the drop coating method deposited on it, then another CaF_2 window was placed on top to secure the loose ND powder between the windows. Note monolayers of ND (as used in the electrical measurements) were not used due to their low IR absorption, resulting in unacceptable signal to noise ratio, therefore the drop coated ND layers were *ca*. 300 nm thick. Both styles of coated CaF_2 window were then mounted in the FTIR with a corresponding (single or double) uncoated reference window from which to compare spectra in order to remove any influence of the CaF_2 window. Mounted samples were then allowed to sit in the N_2 environment to desorb water, measurements were taken after a 10 min N_2 purge. Samples were scanned and an average was calculated over 10 min between 800 and $4000\,cm^{-1}$.

III. RESULTS AND DISCUSSION

A. Nanodiamond surface modification

Figure 1(a) shows the FTIR spectrum of untreated ND. Here, the most striking feature is the wide peak between 3000 and $3600\,cm^{-1}$, which can be attributed to the covalent hydroxl bond from adsorbed water.[18] The narrow peak at $1726\,cm^{-1}$ can be ascribed to the $C=O$ stretch seen in carboxylic acid groups and anhydride functionalities.[19] Between 1000 and $1500\,cm^{-1}$, there is a convoluted set of peaks typical for ND including COO-, C-O-C, C-OH, and C-H.[20] The surface state after hydrogen treatment is shown in Figure 1(b). A significant feature is the strong CH_x stretch centred at $2923\,cm^{-1}$, coupled with the peaks at $1461\,cm^{-1}$
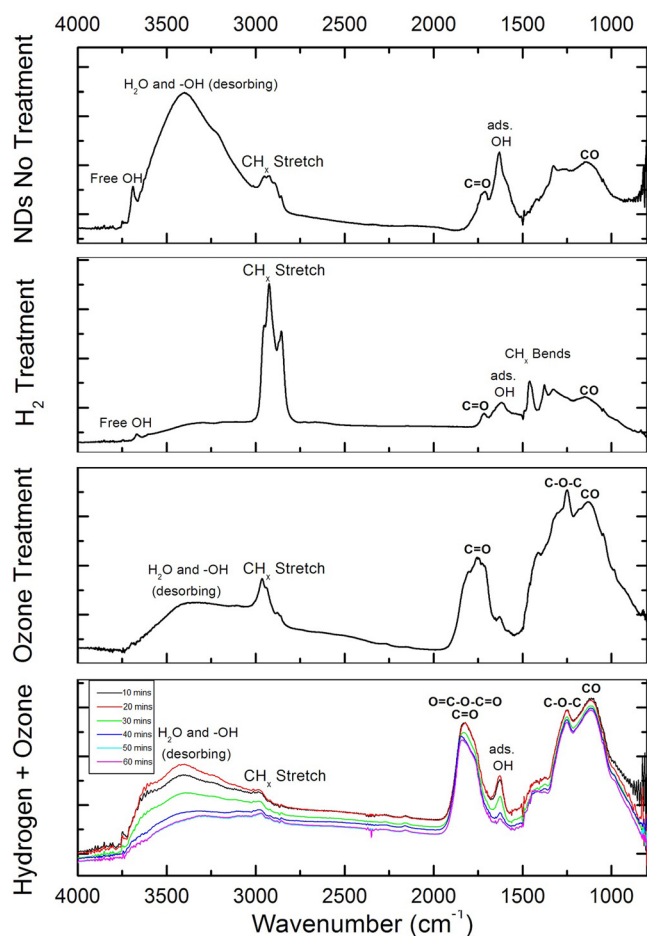

FIG. 1. FTIR spectra taken on (a) as received ND, (b) hydrogen treated ND, (c) ozone treated ND, (d) hydrogen then ozone treated ND with increasing N_2 purge durations.

and $1377\,cm^{-1}$ (CH_2 and CH_3, respectively) which strongly indicate hydrogenation of the diamond surface.[21] Also of note is the reduced occurrence of the $C=O$ stretch at $1726\,cm^{-1}$ in comparison to the untreated surface. The complete absence of the wide peak between 3000 and $3600\,cm^{-1}$ seen in Figure 1(a) can be explained by the hydrophobicity of hydrogen terminated diamond preventing readsorption of water.[22] The remaining oxygen containing groups were likely inaccessible to the hydrogen gas during treatment. Figure 1(c) shows the FTIR spectrum obtained after the ozone treatment. There is a peak at $1755\,cm^{-1}$, the $C=O$ stretch, emerging from the anhydride peak. C-O-C and C-O peaks are seen at $1249\,cm^{-1}$ and $1141\,cm^{-1}$, respectively, indicating oxidation of some bonds. However, the CH_x stretch is still apparent, so a full oxidation of the surface has not taken place.

Figure 1(d) shows the spectra taken after hydrogen and subsequent ozone treatment. A very weak CH_x stretch can now be observed—when compared to the ozone only treatment, there is clearly a greater efficacy of CH_x removal. The band centred around $1800\,cm^{-1}$ (associated with cyclic acid anhydride) is also distinct from that seen on the ozone only treatment. Strong peaks can also be seen at $1256\,cm^{-1}$ and $1123\,cm^{-1}$ corresponding to C-O-C and C-O peaks, respectively. The desorption of water from the surface can be seen

across 3000–3750 cm^{-1} with increasing duration of N$_2$ purges, suggesting a hydrophilic surface—corresponding to oxygen terminated diamond.[22] Hence, the combination of hydrogen and ozone treatments provides well-defined oxygen containing peaks and is preferable to ozone treatment alone. As all samples are dried before or during processing therefore the adsorbed water (or hydrophilicity) seen on the untreated and oxygenated NDs should not be a contributing factor. Instead, the homogenous surface left by the hydrogen treatment seems to provide an easier target for ozone to oxygenate ND, resulting in short treatment durations.

B. Electrical properties of thin ND layers

Here, the term 'thin ND layer' refers to substrates ultrasonically coated with ND to a thickness of approximately 10 nm, as described in previous work.[2] A note on symbols used: Hollow symbols depict measurements made in vacuum, and solid symbols for measurements performed in air.

1. Hydrogen terminated nanodiamond—air measurement

Figure 2(a) shows that the low frequency impedance of the ND films is reduced with rising measurement temperature, although upon returning the ND layer to room temperature, the low frequency impedance largely recovers indicating typical semiconductive behaviour. The primary observation from Figure 2(a) is the low frequency impedance response is three orders of magnitude lower than that seen in untreated ND,[2] at $10^6 – 10^7 \Omega$. This observed drop is likely due to surface transfer doping, as has been reported on ND by other groups recently The recovery of the original room temperature impedance occurs at higher temperatures than the untreated ND layers, a full 24 h after heating to 475 °C for 10 min, no significant permanent change is detected at room temperature. This suggests hydrogen termination provides some protection against the permanent damage inflicted at higher temperatures. Indeed, hydrogen termination of bulk diamond has long been known to stabilise the surface during and after CVD growth, preventing the transition to other phases, such as graphite.[23] However, after one hour of heating to 475 °C it is apparent that upon return to room temperature (RT after 1 h 475 (°C)) the impedance values do not begin to revert to the initially observed impedance levels. Subsequent measurements at room temperature showed no change. Instead the layer remains much like that seen at 475 °C, indicating a permanent structural change has occurred. This temperature of degradation is only slightly lower than that reported by Lee *et al.* for 150–600 nm CVD diamond spheres heated in dry oxygen (450 °C),[24] although the large change in dimensions from the CVD diamond spheres to ND and the increased oxygen content would be antagonistic factors for the onset of thermal oxidation. It should be noted that due to the production method in the work of Lee and co-workers, the surface of CVD diamond spheres were also hydrogen terminated.

Whilst only one semicircular response (and hence only one observed conduction mechanism)[25] could be determined between 30 and 250 °C from the Cole-Cole plots, a second
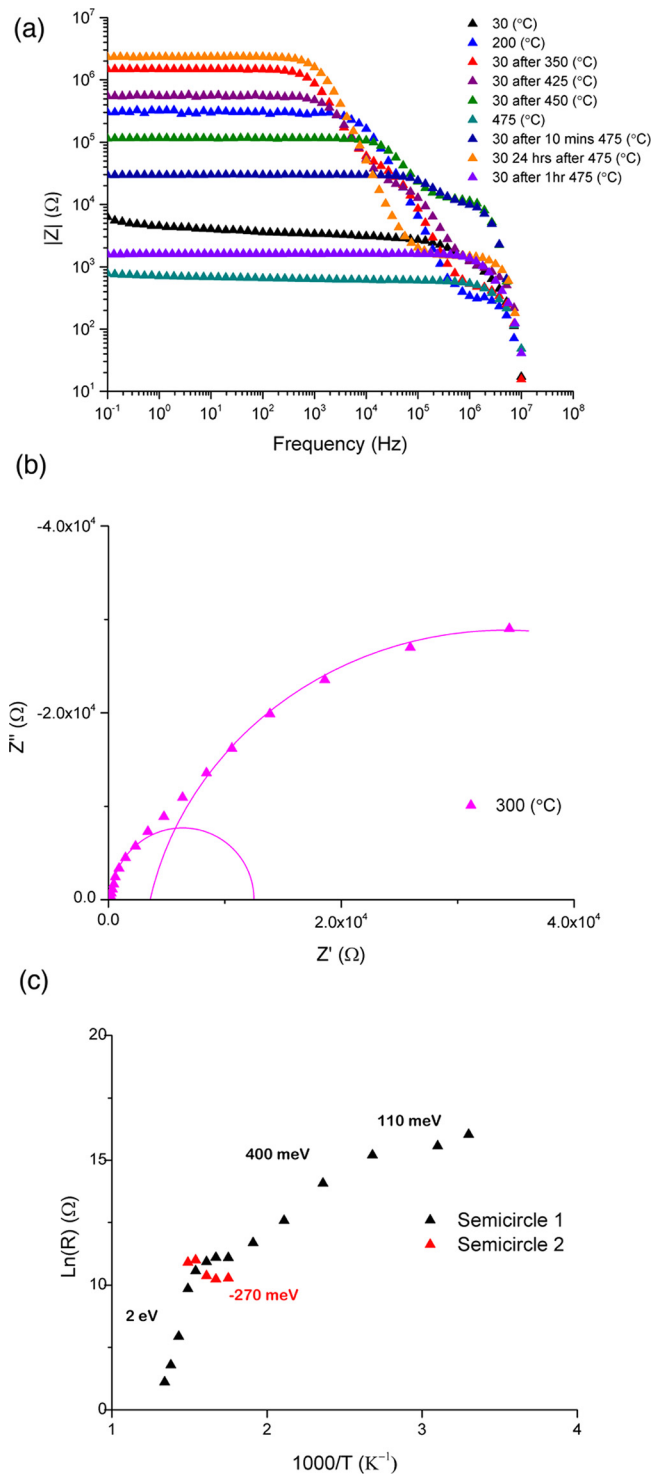

FIG. 2. (a) Bode plot of hydrogen terminated ND in air. Successive cycling between temperatures near the permanent deformation point of untreated ND (seen in Ref. 2) and room temperature were performed to compare temperature stability. (b) Cole-Cole plot of hydrogen terminated ND layer measured at 300 °C. Two semicircular responses are observed and have been fitted to the plot to aid recognition. (c) Arrhenius plot of two conduction paths observed on hydrogen terminated ND layer.

semicircle emerges between 300 and 400 °C (shown in Figure 2(b)). The second conduction path only becomes apparent at temperatures beyond the desorption point of water and other air-bound adsorbates, which are required for surface conductivity. Therefore, this second conduction path cannot be ascribed to hydrogen induced surface conductivity.

However, this second conduction path is maintained once the sample is returned to room temperature. Therefore, this trend could be present at lower temperatures, but masked by the larger, lower frequency semicircle. Figure 2(b) shows the first emergence of the second semicircle at 300 °C and highlights the limit in resolving closely positioned conduction paths. The semicircles fitted to the data presented in Figure 2(b) were determined to show that the capacitance had a magnitude in the tens of picofarads. Picofarad capacitance has been reported previously to indicate grain interior conduction in polycrystalline film (whereas nanofarad capacitance is associated with grain exterior conduction).[26] The magnitude of capacitance in Figure 2(b) lies only one order of magnitude greater than the untreated ND layers indicating a similar, if slightly less ordered, material through which the conduction mechanism passes. Figure 2(c) shows an Arrhenius plot of the extracted semicircular responses seen on a hydrogen terminated ND layer. For the first semicircle, three regimes are apparent. Between 30 and 100 °C $E_a = 110$ meV (Standard error (S.E) = 30 meV), for 100–300 °C $E_a = 400$ meV (S.E = 20 meV), and for 375–475 °C $E_a = 2$ eV (S.E = 130 meV). The second semicircle has a negative activation energy of −270 meV (S.E = 85 meV) between 300 and 400 °C. The low temperature range activation energy is likely due to the removal of the adsorbed wetting layer,[27] which is readsorbed upon return to room temperature. The mid-level activation energy (100–300 °C) is due either to the removal of adsorbed gas (ND has a very high sorption capacity of between 150 and 450 m^2 g^{-1})[28] or just through previously reported, unspecified defects shown to have an activation energy of 400 meV.[29] The activation energy seen above 375 °C is far greater than those previously described. At 2 eV, this activation energy is substantially lower than that given for the removal of hydrogen reported in the literature. A value of ∼80 kcal mol^{-1} (3.47 eV) was found by Su *et al.* through temperature programmed desorption, however, this was performed on {100} oriented bulk diamond at UHV pressures (2×10^{-10} Torr)[30] and hence cannot be easily compared to the present case. Studies on the thermal decomposition of ND (at 10^{-5} Torr) show the onset of CH_x groups' desorption to be *ca.* 750 °C,[31] far above the temperature reached in this experiment. Additionally, the fact the impedance values recover upon return to room temperature (at least when a maximum temperature below 475 °C is used) indicates the hydrogen termination, and hence the surface conductivity, is not lost. Zhao *et al.* calculated the size dependence of the onset of nanodiamond-graphite transition.[32] Their calculations suggest 5 nm ND would undergo graphitisation as low as 425 °C. Indeed, this theoretical prediction was later confirmed by the work of Osswald *et al.* who showed that below 375 °C, oxidation in air was not detected, however, above 450 °C both sp^2 and sp^3 carbon are oxidised. Therefore, the activation energy seen in Figure 2(c) between 375 and 475 °C is likely the oxidation of graphite with a possible contribution from the early stages of diamond oxidation. Finally, the onset of the second semicircle results in an observed negative activation energy suggesting a barrier-less reaction where increasing the temperature decreases the probability

of the excitation of a charge carrier. In isolation, this may be due to de-trapping at defect sites, however, as previously discussed the close proximity of a larger semicircle in Figure 2(b) may be preventing the identification of this trend at lower measurement temperatures.

2. Hydrogen terminated nanodiamond—Vacuum measurement

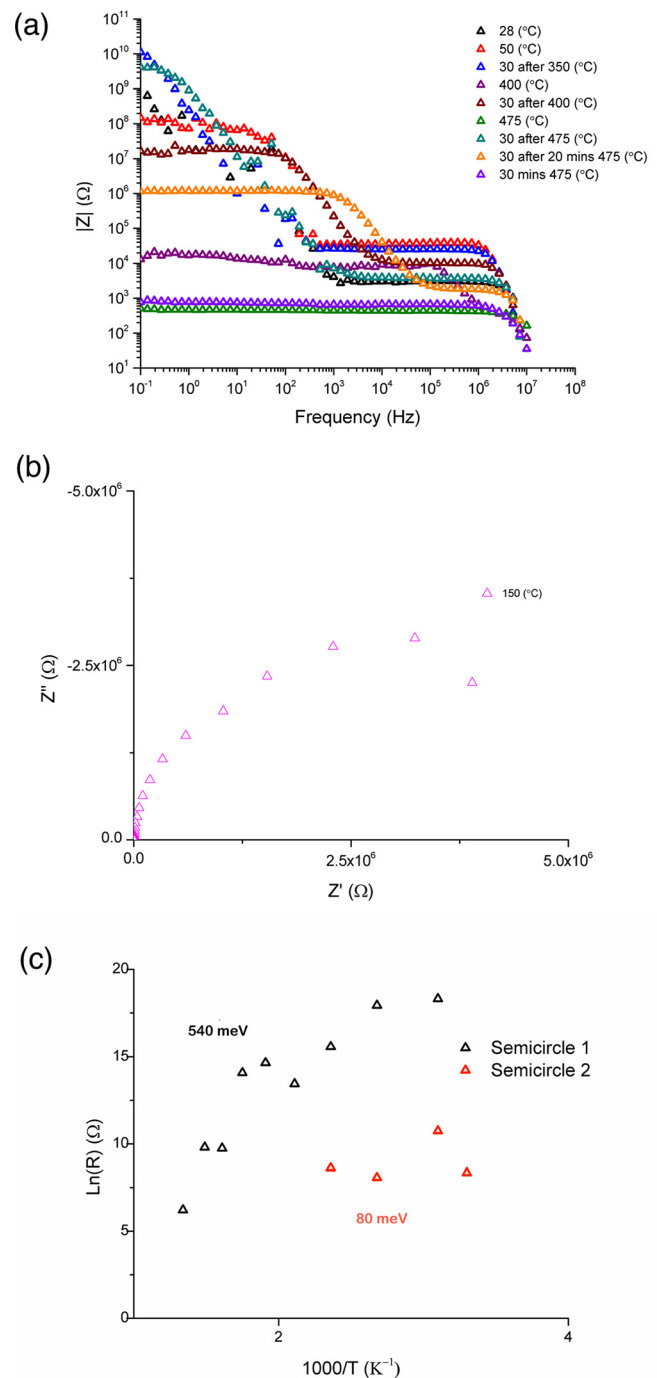Figure 3(a) shows that when the measurements are preformed in a vacuum, the hydrogen-terminated ND layer

FIG. 3. (a) Bode and (b) Cole-Cole plot of hydrogen terminated ND in low vacuum (10^{-3} mbar). For the data presented at 150 °C, two semicircular responses are apparent. (c) Arrhenius plot of primary and secondary conduction paths seen on hydrogen terminated ND measured in vacuum.

displays an extremely high impedance, at 10^{10} Ω, similar to both bulk diamond and aggregated nanodiamond.[33] This is in stark contrast to when measuring hydrogen treated ND in air, as the room temperature impedance is three orders of magnitude lower than that seen in vacuum. As such, the layer more closely resembles the response seen in untreated or oxygen terminated ND layers (see Chaudhary *et al.*[2] and Figure 4(a), respectively). This corroborates the evidence presented in Figure 2(a) of the hydrogen treatment inducing surface transfer doping as this effect is not seen in vacuum due to the removal of necessary surface adsorbates. Above 150 °C, the behaviour of the layers is largely identical, as would be expected of a conduction mechanism that relies on the presence of a wetting layer and adsorbates. In contrast to the data acquired in air, hydrogen terminated ND in vacuum shows two conduction paths below 150 °C. The primary conduction path does not show as great a disparity between vacuum and air measurements in the magnitudes of room temperature impedance (10^{10} and 10^{6} Ω, respectively). Instead, the gap is narrowed to 10^{7} and 10^{6} Ω, so whilst the bode plots indicate similar room temperature behaviour between untreated ND in air and hydrogen terminated ND in vacuum, closer analysis of the data reveals this relationship only holds for the absolute magnitude of impedance. Interestingly, the second conduction path in vacuum is of the same order of magnitude as that seen above 300 °C in air, lending weight to the earlier proposition that a second conduction path does exist below 300 °C in air, buried by a closely situated semicircle. Both vacuum and air measurements show the second semicircle to remain upon return to room temperature. The Arrhenius plot of the extracted semicircular responses seen on a hydrogen terminated ND layer measured in vacuum is presented in Figure 3(c). Due to the noise observed, it is difficult to ascertain whether the primary semicircle is one regime or more. Fitting the entire range yields $E_a = 540$ meV (S.E = 94 meV) between 30 and 475 °C. There is a greater incidence of noise around the second semicircle where between 30 and 150 °C $E_a = 80$ meV with a rather high standard error (S.E = 170 meV), making it difficult to draw firm conclusions from these Arrhenius plots.

3. Oxygen terminated nanodiamond—Air measurement

Figure 4(a) indicates the difficulty in performing a stable measurement on oxygen terminated ND in air. The data are initially noisy at room temperature, and then beyond a temperature of 150 °C further measurements were not possible due to the sample becoming too conductive. Therefore, it was ascertained that permanent damage had occurred through the ND layer at a far lower temperature (200 °C) than that seen on either the untreated or hydrogen terminated samples. The sample was subsequently slowly cooled and measurements taken at regular temperature intervals to investigate at what point the sample became measureable again. It was found the oxygen terminated ND had a far lower impedance, approximately 10^{5} Ω, and this was only weakly temperature dependent. This difficulty is likely due to the oxygen termination hastening the onset of
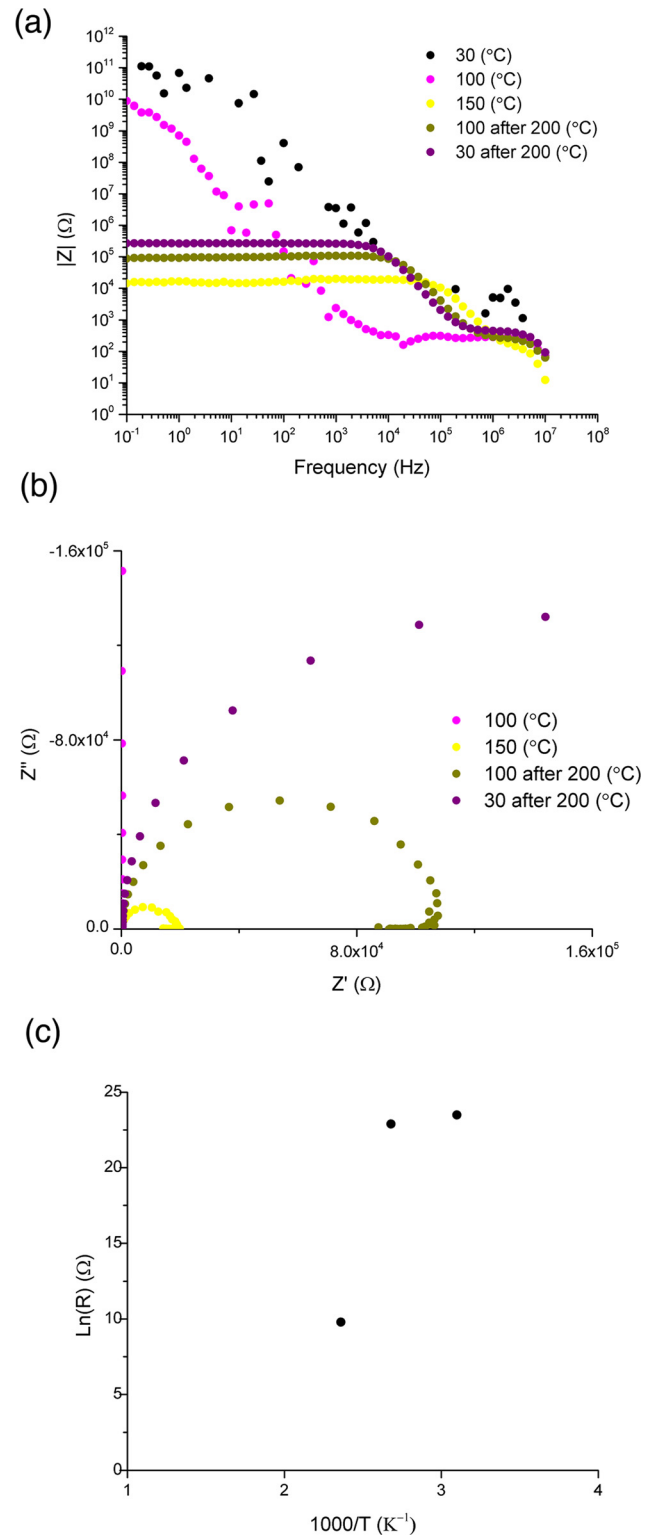

FIG. 4. (a) Bode plot, (b) Cole-Cole plot, and (c) Arrhenius plot of oxygen terminated ND, measured in air. Note the lack of a sufficient number of data points to calculate an activation energy.

graphitisation, possibly accelerated through the increased presence of adsorbed water (see Figure 1(d)) due to the hydrophilic nature of oxygen terminated ND. Previous studies have shown water to act as a catalyst for the graphitisation of 40–60 nm ND particles in high pressure high temperature conditions (2 GPa, 785–1485 °C),[34] therefore, it

is likely that this mechanism is amplified for smaller particles and hence this effect could be observed at ambient pressure and a temperature of 200 °C. The oxygen in the air also has an effect; Danilenko reported the exclusion of oxygen caused a three orders of magnitude shift in rates of graphitisation over a 22 year period at room temperature.[35] This work found the shells of NDs were first graphitised, then oxidised leaving a smaller core size of ND. This process would continue until the ND reached a core size around 4 nm where a dramatic graphitisation of the entire particle would take place. This process reportedly occurred at 525 °C, higher than the temperatures used in the current study, however it is likely that this process is occurring, albeit at a reduced rate. This might provide insight into why at high temperature the ND layer is too conductive to measure—the thermal activation of carriers as seen in the untreated and hydrogen terminated ND, combined with the graphitisation of the ND shell, causes effective conduction routes through the ND layer, causing a collapse in measured impedance. Upon return to sub-critical temperatures (i.e., 100 °C) the removal of the thermally activated carriers leaves the ND layer with an impedance response between that of pure ND (or bulk diamond) and graphite, where the isolated graphitic regions do not yet form a continuous conduction path. Figures 4(a) and 4(b) show the single semicircular response indicating a single conduction path is seen for oxygen terminated ND layers. The measurements that were achieved showed a wide range of resistance values associated with the fitted semicircles in a very narrow temperature window— 10^{10} Ω for 50 °C, and 10^3 Ω for 150 °C. The data points displayed in Figure 4(c) are insufficient to draw firm conclusions from, however, the extent of the slope appears to be of the order of magnitude associated with graphitisation.

4. Oxygen terminated nanodiamond—Vacuum measurement

Figure 5(a) shows IS data for oxygen terminated NDs measured in vacuum. An initial impedance of 10^8 Ω can be seen, 2–3 decades lower than that observed at atmospheric pressure. This lies close to the initial impedance seen on hydrogen terminated diamond when measured in vacuum and may be due to the removal of surface adsorbates that aid conduction through the wetting layer, as after heating and once the ND layer has had 18–24 h to recover, the impedance is an order of magnitude higher than the initial value. This recovery behaviour is distinct to the previous experiments, where permanent change to the impedance was observed. In this case, the overall increase in impedance suggests the heating and cooling stages are removing graphitic deposits. Figure 5(b) depicts the recovery of impedance after several heating and cooling cycles. Both sets of data exhibit a high degree of noise, however semicircle fits before and after exposure to 475 °C yield extracted resistance values only one order of magnitude apart. All extracted capacitance values are of the 10 pF order of magnitude, indicating crystalline material remains.[23] At the peak temperature, the only conduction path seen was *ca.* 5 kΩ (C = 95 pF), however when measured immediately after return to room
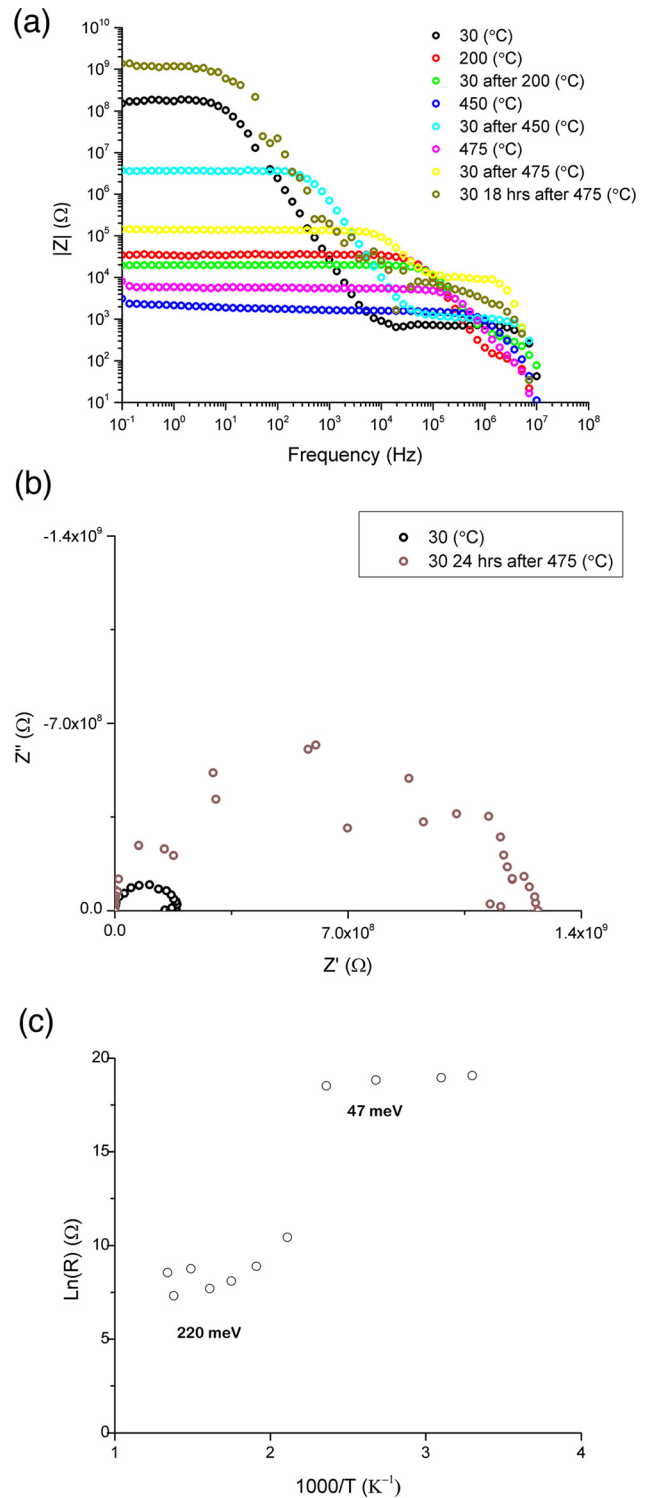

FIG. 5. (a) Bode plot of oxygen terminated ND in vacuum. Successive cooling stages were performed in an attempt to find the temperature where permanent reduction of the impedance occurs. Additionally, a large cooling period was performed to investigate the recovery of impedance at room temperature. (b) Cole-Cole plots of original and recovered impedance values (c) Arrhenius plot of the extracted conduction path resistance values, taken on oxygen terminated ND layers in vacuum.

temperature (25 min later) two conduction paths were visible, with the primary at 3×10^8 Ω (C = 88 pF) and the secondary at 10 kΩ (C = 5 pF). The observed shift in capacitance was the only observed occurrence, this effect

was not seen after further time at room temperature. Therefore, considering the noise on the data, and the single occurrence, it is difficult to draw firm conclusions from this observation. The Arrhenius plot in Figure 5(c) resembles that of untreated ND measured in air, with two distinct regions separated by a sudden shift in extracted resistance at 200 °C. For the first region between 30 and 150 °C, $E_a = 47$ meV (S.E = 8.5 meV), whereas for the second high temperature region between 200 and 475 °C, $E_a = 220$ meV (S.E = 96 meV). Neither value for E_a is of the order expected for ND graphitisation, suggesting only desorption and oxidation processes occurring on the oxygen terminated ND layer.

IV. CONCLUDING REMARKS

The electrical properties of NDs have been explored as a function of H- or O- terminations. Despite NDs being prone to phase changes on heating to far more modest temperatures than bulk diamond, the fact that so-called surface transfer-doping can be observed on NDs when hydrogenated suggests conditions exist where they can be electrically similar to bulk diamond. This important observation means that surfaces coated with H-terminated NDs can be expected to display properties expected of H-terminated bulk diamond. Given that 3D ND coatings can be simply produced from water-based room temperature sonication processes, many new applications for diamond coatings on materials that would not be stable under conventional diamond CVD conditions can be envisaged.

The acquisition of FTIR required very thick layers to be treated in order to obtain enough material for the transmission experiments, however, this is sub-optimal for static dry processing as some ND material will not be exposed to the reactants and therefore the observed changes to the ND surface may be underestimated, particularly when compared to the thin ND films presented here. Therefore, it is reasonable to suggest the spectra shown in Figure 1 may be understating the effect of processing on thin ND layers. During the temperature cycling, the electronic properties of hydrogen terminated ND particles recover after short exposures to high temperature (475 °C). However, the observation that this is lost with greater durations of heating (1 h), leading to behaviour similar to that seen on oxygen terminated ND, suggests hydrogen terminations are gradually replaced by oxygen containing groups from the atmosphere (in the case of air measurements). This process is not observed in vacuum, reinforcing the notion the ambient air—likely the oxygen and moisture content—plays a vital role in the degradation of the electronic properties. Oxygen terminated ND is seen to degrade at a far lower temperature threshold (200 °C) in air. This is likely mediated through its hydrophilicity,[17] where OH ions are free to attack oxygen containing surface groups, occasionally resulting in the formation of dangling bonds, which are thought to be required for the graphitisation of the surface.[36] Perhaps the most surprising result was the extremely resilient behaviour of the NDs, particularly in vacuum. The ubiquitous occurrence of picofarad magnitude capacitance throughout the sample series suggests the conduction paths observed are associated with grain

interiors.[23] Whilst surface treatments certainly modulate the number of charge carriers present, this study indicates the bulk of charge transfer occurs within the ordered sp³ interior of the ND, not the mixed phase surface. When surface transfer doping is not present (i.e., oxygen terminated ND) capacitance values of the order of tens of picofarads are observed, suggesting conduction through the outer sp³ regions where higher concentrations of defects are present at the interface between the core and shell of the ND[37] but not through the grain boundary where nanofarad magnitude capacitance is expected.[23]

[1]S. Szunerits and R. Boukherroub, J. Solid State Electrochem. **12**, 1205 (2008).
[2]A. Krüger, F. Kataoka, M. Ozawa, T. Fujino, Y. Suzuki, A. E. Aleksenskii, A. Ya. Vul, and E. Ōsawa, Carbon **43**, 1722 (2005).
[3]A. Chaudhary, J. O. Welch, and R. B. Jackman, Appl. Phys. Lett. **96**, 242903 (2010).
[4]O. A. Williams and R. B. Jackman, Semicond. Sci. Technol. **18**, S34 (2003).
[5]F. Maier, M. Riedel, B. Mantel, J. Ristein, and L. Ley, Phys. Rev. Lett. **85**, 3472 (2000).
[6]D. P. Malta, J. B. Posthill, T. P. Humphreys, R. E. Thomas, G. G. Fountain, R. A. Rudder, G. C. Hudson, M. J. Mantini, and R. J. Markunas, Appl. Phys. Lett. **64**, 1929 (1994).
[7]T. Kondo, I. Neitzel, V. N. Mochalin, J. Urai, M. Yuasa, and Y. Gogotsi, J. Appl. Phys. **113**, 214307 (2013).
[8]J. B. Cui, J. Ristein, and L. Ley, Phys. Rev. Lett. **81**, 429 (1998).
[9]M. Karlsson, P. Forsberg, and F. Nikolajeff, Langmuir **26**, 889 (2010).
[10]S. Zeppillia, J. C. Arnault, C. Gesset, P. Bergonzo, and R. Polini. Diamond Relat. Mater. **19**, 846 (2010).
[11]S. Su, J. Li, V. Kundrát, A. M. Abbot, and H. Ye, J. Appl. Phys. **113**, 023707 (2013).
[12]S. Nath and J. Wilson, "Impedance measurements on CVD diamond," Diamond Relat. Mater. **5**, 65 (1996).
[13]S. Curat, H. Ye, O. Gaudin, R. B. Jackman, and S. Koizumi, J. Appl. Phys. **98**, 073701 (2005).
[14]N. Tumilty, J. Welch, H. Ye, R. S. Balmer, C. Wort, R. Lang, and R. B. Jackman, Appl. Phys. Lett. **94**, 052107 (2009).
[15]H. El-Hajj, A. Denisenko, A. Bergmaier, G. Dollinger, M. Kubovic, and E. Kohn, Diamond Relat. Mater. **17**, 409 (2008).
[16]E. Osawa, Pure Appl. Chem. **80**, 1365 (2008).
[17]See http://www.solartronanalytical.com/material-test-systems/model-1296a-dielectric-interface-system.aspx for Solartron 1296A, Solartron, accessed 13th June 2013.
[18]T. Jiang and K. Xu, Carbon **33**, 1663 (1995).
[19]P. H. Chung, E. Perevedentseva, J. S. Tu, C. C. Chang, and C. L. Cheng, Diamond Relat. Mater. **15**, 622(2006).
[20]C. D. Chu, E. Perevedentseva, V. Yeh, S. J. Cai, J. S. Tu, and C. L. Cheng, Diamond Relat. Mater. **18**, 76 (2009).
[21]C. L. Cheng, C. F. Chen, W. C. Shaio, D. S. Tsai, and K. H. Chen, Diamond Relat. Mater. **14**, 1455 (2005).
[22]L. Ostrovskaya, V. Perevertailo, V. Ralchenko, A. Dementjev, and O. Loginova, Diamond Relat. Mater. **11**, 845 (2002).
[23]H. Kawarada, Surf. Sci. Rep. **26**, 205 (1996).
[24]J. K. Lee, M. W. Anderson, F. A. Gray, P. John, J. Y. Lee, Y. J. Baik, and K. Y. Eun, Diamond Relat. Mater. **13**, 1070 (2004).
[25]P. Vanýsek, DTIC Report No. AD-A277081, 78 (1994).
[26]L. Hench and J. West, *Principles of Electronic Ceramics* (Wiley, 1990), Chap. 5.
[27]V. Pichot, M. Comet, E. Fousson, C. Baras, A. Senger, F. Le Normand, and D. Spitzera, Diamond Relat. Mater. **17**, 13 (2008).
[28]I. I. Kulakova, Phys. Solid State **46**, 636 (2004).
[29]V. Mortet, J. D'Haen, J. Potmesil, R. Kravets, I. Drbohlav, V. Vorlicek, J. Rosa, and M. Vanecek, Diamond Relat. Mater. **14**, 393(2005).
[30]C. Su and J. Lin, Surf. Sci. **406**, 149 (1998).
[31]V. Kuznetsov and Y. Butenko, *Synthesis and Applications of Ultrananocrystalline* (Diamond, Springer, Dordrecht, 2005), Vol. 15, p. 199.
[32]D. S. Zhao, M. Zhao, and Q. Jiang, Diamond Relat. Mater. **11**, 234 (2002).

[33]M. Bevilacqua, S. Patel, A. Chaudhary, H. Ye, and R. B. Jackman, Appl. Phys. Lett. **93**, 132115 (2008).

[34]C. Pantea, J. Gubicza, T. Ungar, G. A. Voronin, and T. W. Zerda, Phys. Rev. B **66**, 094106 (2002).

[35]V. V. Danilenko, J. Superhard Mater. **31**, 218 (2009).

[36]L. Li and X. Zhao, J. Chem. Phys. **134**, 044711 (2011).

[37]V. N. Mochalin, O. Shenderova, D. Ho, and Y. Gogotsi, Nat. Nanotechnol. **7**, 11(2011).